SIX-DIMENSIONAL WEAK-STRONG SIMULATIONS OF HEAD-ON BEAM-BEAM COMPENSATION IN RHIC*

Y. Luo, W. Fischer, N. P. Abreu, X. Gu, A. Pikin, G. Robert-Demolaize
Brookhaven National Laboratory, Upton, NY 11973, USA

Abstract

To compensate the large beam-beam tune spread and beam-beam resonance driving terms in the polarized proton operation in the Relativistic Heavy Ion Collider (RHIC), we will introduce a low energy DC electron beam into each ring to collide head-on with the opposing proton beam. The device to provide the electron beam is called an electron lens. In this article, using a 6-D weak-strong beam-beam interaction simulation model, we investigate the effects of head-on beam-beam compensation with electron lenses on the proton beam dynamics in the RHIC 250 GeV polarized proton operation. This article is abridged from the published article [1].

INTRODUCTION

To further increase the luminosity in the RHIC polarized proton (p-p) run, we plan to increase the proton bunch intensity with an upgraded polarized proton source [2]. In the 2012 RHIC 250 GeV p-p run, the maximum bunch intensity at the beginning of physics store was 1.7×10^{11}. With the upgraded polarized proton source, we expect the maximum bunch intensity will be increased up to 3.0×10^{11}. Assuming the normalized rms transverse emittance 15 π mm.mrad, the linear incoherent tune shift or the beam-beam parameter will reach 0.03.

Currently the working tune space for the RHIC p-p operation is chosen between 2/3 and 7/10 to achieve a good beam lifetime at store with beam-beam interaction and to maintain the proton polarization on the energy ramp and at the physics store [3]. 7/10 is not only a 10th betatron resonance but also a spin depolarization resonance. Therefore, there is not enough tune space between 2/3 and 7/10 to hold the beam-beam generated tune spread when the bunch intensity is bigger than 2×10^{11}.

To reduce the beam-beam tune spread and also to compensate the nonlinear beam-beam resonance driving terms, we planned to install head-on beam-beam compensation in the RHIC p-p operation. The proton beams collide at IP6 and IP8. A DC low energy electron beam will be introduced into each ring around IP10 to head-on collide with the proton beam. The electron beam should have the same transverse profile as the proton beam. The device to provide the electron beam for this purpose is called an electron lens (e-lens) [4].

In the following, with the 6-D weak-strong simulation, we study the head-on ebam-beam compensation with e-lenses on the proton beam dynamics in the RHIC 250 GeV p-p runs. The results from dynamic aperture and proton beam loss rate calculations are presented. Key beam parameters involved in this scheme are varied to search for the optimum compensation condition. The sensitivity of head-on beam-beam compensation to beam imperfections and beam offsets are also studied.

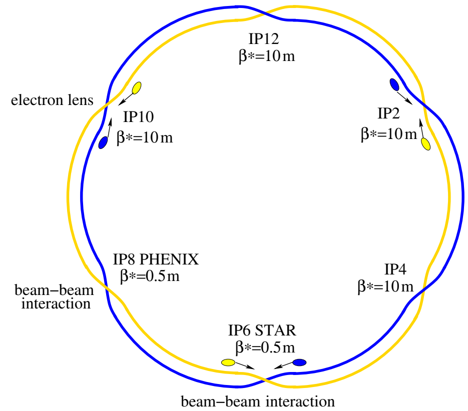

Figure 1: Layout of head-on beam-beam compensation in RHIC. E-lenses are to be installed on either side of IP10.

LATTICE AND BEAM PARAMETERS

In the following simulation, we use a proposed Blue ring lattice for 250 GeV RHIC polarized proton operation. Table 1 lists the lattice and beam parameters. The β^*s at the IP6 and IP8 are 0.5 m. The βs at the e-lenses are 10 m. RHIC has not yet operated with $\beta^* = 0.5$ m. In the 2012 RHIC 250 GeV polarized proton run we achieved $\beta^* = 0.65$m. In this study, we assume that the rms transverse emittance as 15 π mm.mrad and the rms relative momentum spread 1.4×10^{-4}.

To better cancel the nonlinear beam-beam resonance driving terms (RDTs), the betatron phase advance between the beam-beam interaction and the e-lens should be $k\pi$, k is an integer. Since we only have one e-lens for each ring in the current design, we would like to have the betatron phase advances between IP8 and the e-lenses to be $k\pi$. For the above lattice, the default phase adavances between IP8 and the e-lens are (8.5π, 11.1π). In the following study, we will insert an artificial phase shifting matrix to bring them to (9π, 11π).

For simplicity, we define that half and full beam-beam compensation compensate the half and full total linear incoherent beam-beam tune shift. Their compensation strengths are 0.5 and 1 respectively. If the electron beam

* This work was supported by Brookhaven Science Associates, LLC under Contract No. DE-AC02-98CH10886 with the U.S. Department of Energy.

Table 1: Lattice and beam parameters used in this study.

Parameter	Value
Circumference	3833.8451 m
Energy	250 GeV
Working point	$(28.67, 29.68)$
Linear chromaticities	$(1, 1)$
Second order chromaticities	(2800, 2900)
Trans. rms emittance	2.5 mm·mrad
$\beta^*_{x,y}$ at IP6 / IP8	0.5 m
$\beta_{x,y,e-lens}$ at the e-lens	10 m
Trans. rms beam size at IP6 and IP8	68 μm
Trans. rms beam size at e-lens	310 μm
$\Delta\Phi_{x,y}$ between IP6 and IP8	$(10.6\pi, 9.7\pi)$
$\Delta\Phi_{x,y}$ between IP8 and e-lens	$(8.5\pi, 11.1\pi)$
RF harmonic number	360
RF cavity voltage	300 kV
Longitudinal rms bunch area	0.17 eV·s
Bucket height	1.1×10^{-3}
Relative rms momentum spread	1.4×10^{-4}
Rms bunch length	0.45 m

has the same transverse rms beam size as the proton beam at the e-lens, we have $N_e^* = N_p$ and $N_e^* = 2N_p$ for half and full beam-beam compensation respectively. Here N_e^* and N_p are the electron population in the e-lens and the proton bunch intensity.

SIMULATION MODEL

In the following simulation study, we track the proton particles element by element [5]. The non-linear magnetic field errors in the triplets and separation dipoles in the interaction regions are included. Each magnetic element is modeled with a 6-D symplectic transfer map. We adopted the 4th order symplectic integration [6]. To save time in the long-term particle tracking, we model the magnetic multipoles as thin lens kicks. Tunes and chromaticities are rematched before tracking.

Considering that β^* is comparable to the proton bunch length, we use the 6-D weak-strong synchro-beam map [7] to model the proton-proton beam-beam interaction at IP6 and IP8. The strong bunch is split into 11 slices to achieve good convergence. Considering that the e-lens is working in a DC mode, its electric and magnetic fields are static. In the simulation code, we split the 2 m long e-lens into 8 slices. Each slice is modeled as a drift – a 4-D weak-strong beam-beam kick – a drift. The 4-D weak-strong beam-beam kick is given by Bassetti and Erskine [8].

To fully use the available tune space between 2/3 and 7/10 and for better comparison of the simulation results under different beam-beam conditions, we fix the zero-amplitude particle tunes at (0.67, 0.68) under different beam-beam conditions, except in the proton working point scan. The RHIC polarized proton operation experience shows that a lower working point between 2/3 and 7/10 is preferable to obtain a better beam-beam lifetime and to preserve the proton polarization at store. In the simulation, the linear chromaticities are set to (1,1).

DYNAMIC APERTURE CALCULATION

In this section, we calculate the proton dynamic aperture with head-on beam-beam compensation in RHIC. Particles are tracked in 10 phase angles in (x, y) plane up to 10^6 turns. The initial relative momentum error is 0.42×10^{-4}. We compare the minimum dynamic aperture under different beam and lattice conditions. The dynamic aperture is given in units of rms transverse beam size σ.

Figure 2 shows the dynamic apertures without, with half, and full head-on beam-beam compensation. The proton bunch intensity varies from 1.0×10^{11} to 3.0×10^{11}. In this calculation, the betatron phase advances between IP8 and the e-lens are the default ones (8.5π, 11.1π). From Figure 2, half beam-beam compensation increases the dynamic aperture when the proton bunch intensity is bigger than 2.0×10^{11}. Full beam-beam compensation reduces the dynamic aperture for all shown bunch intensities.

Figure 3 shows the dynamic apertures versus the head-on beam compensation strength. In this study, we keep the electron transverse beam size same as the proton beam size at the e-lens, and adjust the electron beam intensity to change the beam-beam compensation strength. From Figure 3, the proton dynamic apertures sharply drop when the compensation strength is larger than 0.7. The optimized compensation strengths for the bunch intensities 2.5×10^{11} and 3.0×10^{11} are around 0.5-0.6.

Figure 4 shows the dynamic apertures of half head-on beam-beam compensation with $k\pi$ phase advances between IP8 and the e-lens and the second order chromaticity correction. The second order chromaticities without correction are around 2800. With correction, they are below 500. The results show that the $k\pi$ phase advances and second order chromaticity further improve the dynamic aperture of half beam-beam compensation by about 1 σ for all the bunch intensities shown in the plot.

In the above calculation, the zero-amplitude tunes of the proton beam are fixed at (0.67, 0.68). With beam-beam compensation, the tune footprint becomes smaller and it is possible to scan the proton working point between 2/3 and 7/10 to maximize the dynamic aperture with a better working point. Figures 5 and 6 show the dynamic apertures of half and full beam-beam compensation in the tune scan. The horizontal axis is the fractional horizontal zero-amplitude tune. The fractional vertical zero-amplitude tune is always 0.01 higher than the horizontal one. Simulation results show that half beam-beam compensation prefers a lower working point between 2/3 and 7/10, while full beam-beam compensation prefers a higher working point. The maximum dynamic aperture of half beam-beam compensation in the tune scan is higher than that with full beam-beam compensation.

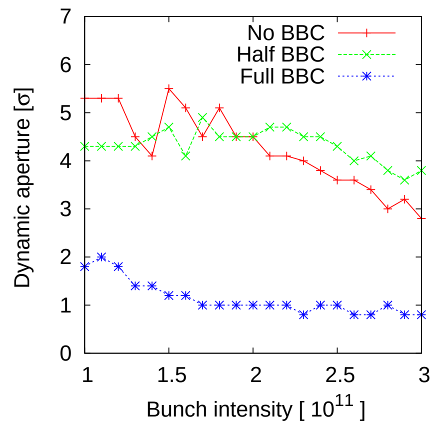

Figure 2: Dynamic apertures without beam-beam compensation and with half and full beam-beam compensation.

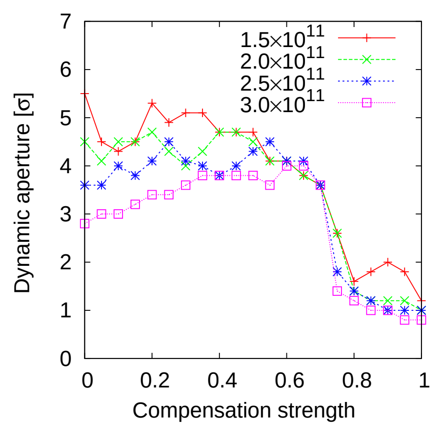

Figure 3: Dynamic apertures of four proton bunch intensities versus head-on beam-beam compensation strength.

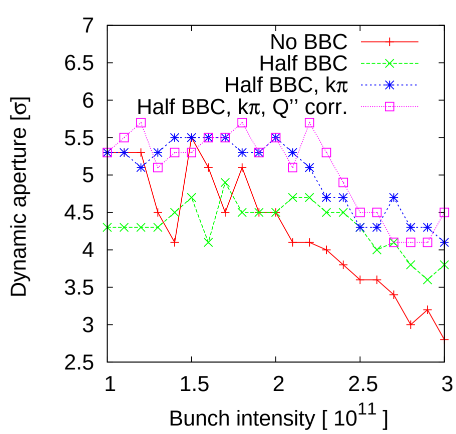

Figure 4: Dynamic apertures of half head-on beam-beam compensation with the betatron phase advance adjustment and the global second order chromaticity correction.

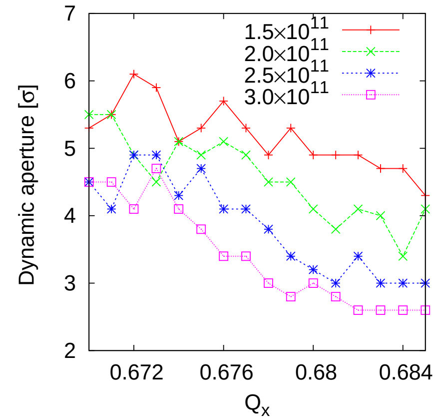

Figure 5: Dynamic apertures of half head-on beam-beam compensation in the scan of proton working point.

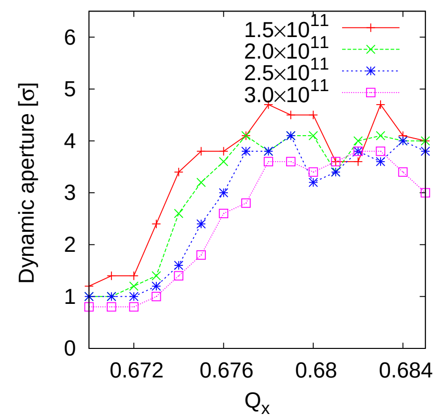

Figure 6: Dynamic apertures of full head-on beam-beam compensation in the scan of proton working point.

PARTICLE LOSS RATE CALCULATION

In this section, we calculate the proton beam loss rate with multi-particle tracking in the presence of head-on beam-beam compensation. Limited by computing capacity, in most cases we track 4800 macro-particles up to 2×10^6 turns. 2×10^6 turns are 24 seconds for RHIC.

Particles with large transverse amplitudes and large momentum deviations are likely lost in long-term tracking. However, for a limited number of macro-particles sampled from a solid Gaussian distribution, there are only a few macro-particles in the Gaussian bunch tail. To detect a small beam loss in 2×10^6 turns without increasing the number of macro-particles, we track particles with an initial hollow Gaussian distribution.

In this approach, we assume that the particles in the bunch core are stable and will not be lost in 2×10^6 turns. To save computing time, we only track macro-particles whose transverse or longitudinal amplitudes are bigger than a certain rms beam size. The boundary between the stable core and the unstable bunch tail is carefully cho-

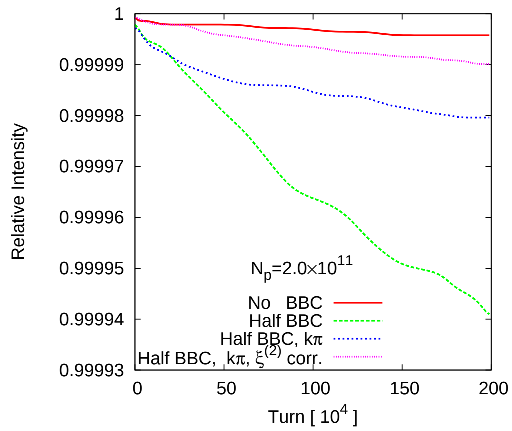

Figure 7: Relative proton beam losses in 2×10^6 turns for the proton bunch intensity 2.0×10^{11}.

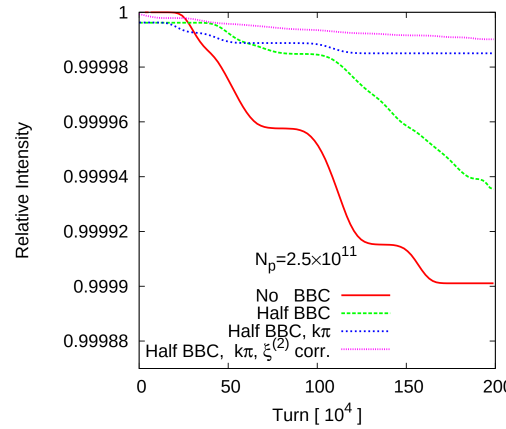

Figure 8: Relative proton beam losses in 2×10^6 turns for the proton bunch intensity 2.5×10^{11}.

sen. We first calculate the dynamic aperture and set the boundary well below it.

Figures 7-9 show that the relative proton beam losses in 2×10^6 turns under different beam-beam compensation conditions with proton bunch intensities 2.0×10^{11}, 2.5×10^{11}, and 3.0×10^{11}. Same as in the dynamic aperture calculation, here we set the zero-amplitude tunes of the proton beam to (0.67, 0.68) and the linear chromaticities (1,1).

For each proton bunch intensity, we compare the relative proton beam losses without beam-beam compensation, with half beam-beam compensation, with the optimized betatron phase advances $k\pi$ between IP8 and the e-lens, and with the global second order chromaticity correction. For all the three bunch intensities, full head-on beam-beam compensation gives a much bigger beam loss than other beam-beam conditions and therefore its beam loss is not plotted.

From Figures 7-9, half head-on beam-beam compensation reduces proton particle losses with bunch intensities 2.5×10^{11} and 3.0×10^{11} in 2×10^6 turns. And the $k\pi$ phase advances between IP8 and the e-lens and the second order chromaticity correction further improve the proton beam lifetime, which agrees the results from above dynamic aperture calculations. For the bunch intensity 2.0×10^{11}, simulation shows that head-on beam-beam compensation does not increase the proton lifetime.

SENSITIVITY STUDY

In this section, we study the sensitivity of head-on beam-beam compensation to the beam imperfections and beam noise. We focus on the Gaussian tail truncated electron beam, the random noise in the electron beam current, and the static and random offsets between the electron and proton beams. The baseline for this study is with the proton bunch intensity $N_p = 2.5 \times 10^{11}$ and half half beam-beam compensation. The betatron phase advance adjustment and

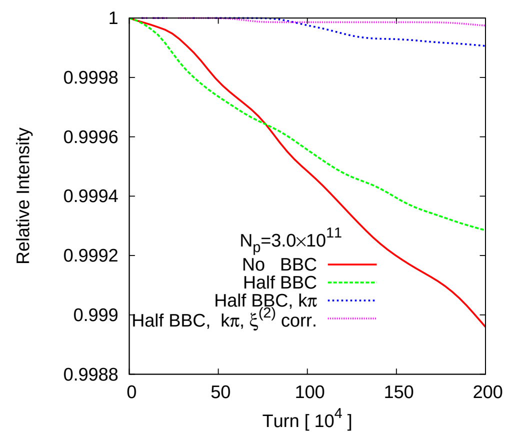

Figure 9: Relative proton beam losses in 2×10^6 turns for the proton bunch intensity 3.0×10^{11}.

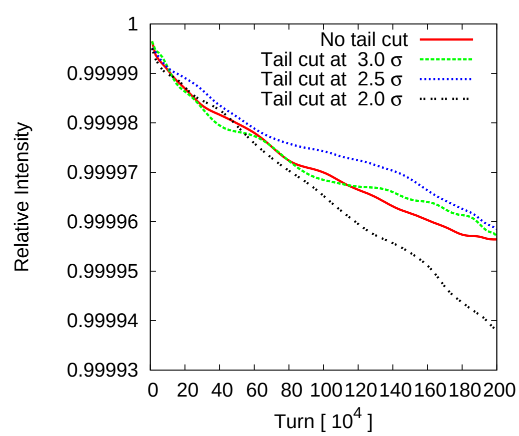

Figure 10: Relative proton beam loss with the truncated Gaussian tail of the electron beam.

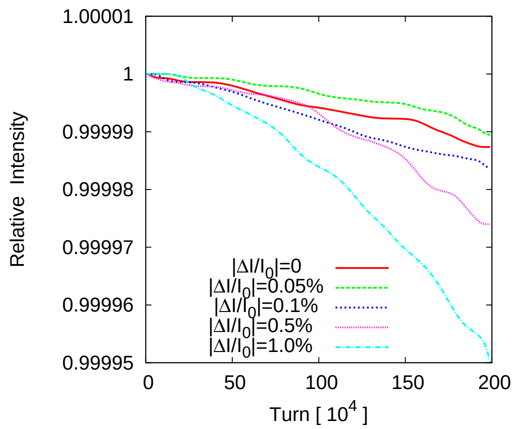

Figure 11: Relative proton beam loss versus the random noise in the electron beam current.

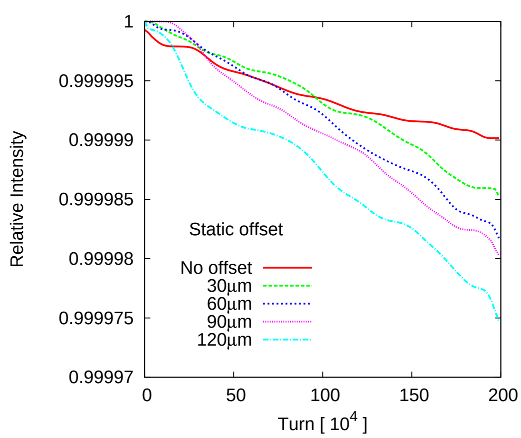

Figure 12: Relative proton beam loss with static transverse offset between the e-lens and the proton beam in the e-lens.

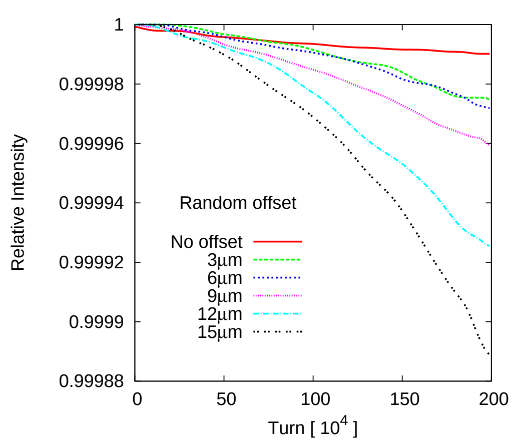

Figure 13: Relative proton beam loss with random transverse offset between the e-lens and the proton beam in the e-lens.

second order chromaticity correction are included.

In the above simulation study, we assume that the electron beam has a perfect transverse Gaussian distribution. Simulation of the electron gun for the RHIC e-lens system shows that the electron beam has a Gaussian tail cut off at 2.8 σ. Figure 10 shows the calculated relative proton beam loss with the electron beam's Gaussian tail cut off at 3 σ, 2.5 σ and 2 σ. Comparing to the baseline with a prefect Gaussian distribution, the Gaussian tail cut at 2.8 σ from the current electron gun design is acceptable.

Due to the instability of the power supplies of the electron gun, there is noise in the electron beam current. Figure 11 shows the relative proton beam loss versus the random electron current noise. The proton beam loss with a random noise below 0.1% in the electron current is comparable to the baseline without current noise. In the design of the RHIC electron gun system, we require that the stability of the power supplies of the electron gun should be better than 0.1%.

Over-lapping of the electron and proton beams in the e-lens plays a crucial role in the head-on beam-beam compensation. Figures 12 and 13 show the calculated relative proton beam losses with static and random offsets between the electron and proton beams. Based on the simulation results, in the RHIC e-lens design, we set the tolerance of the static offset error to 30 μm which is a tenth of a rms beam size in the e-lens and the random offset to 9 μm, which requires the stability of the bending magnet's power supply better than 0.01%.

SUMMARY

In this article, with a 6-D weak-strong beam-beam model, we investigated the effects of head-on beam-beam compensation with e-lenses on the proton beam dynamics in the RHIC 250 GeV p-p operation. We found that half beam-beam compensation improves the proton dynamic aperture and beam lifetime. The $k\pi$ phase advances between IP8 and the e-lens and the global second order chromaticity further increase the proton dynamic aperture and particle loss rate. The sensitivity of half beam-beam compensation on the electron profile, electron current, and the over-lapping of electron and proton beams are studied and their tolerances are set.

REFERENCES

[1] Y. Luo, W. Fischer, et al., Phys. Rev. ST Accel. Beams 15, 051004 (2012).

[2] A. Zelenski, Rev. Sci. Instrum. 81, 02B308 (2010).

[3] M. Bai, et al., Phys. Rev. Lett. 96, 174801 (2006)

[4] V. Shiltsev, et al., Rev. Lett. 99, 244801 (2007).

[5] Y. Luo, in Proceedings of the 2010 IPAC'10, Kyoto, Japan.

[6] R.D. Ruth, IEEE Trans. Nucl. Sci., vol. NS-30, PP.2669-2671 (1983).

[7] K. Hirata, et al., Particle Accel. 40 (1993) 205-228.

[8] M. Bassetti and G.A. Erskine, CERN-ISR-TH/80-06.